JOURNAL OF CATALYSIS 98, 221–228 (1986)

Catalytic Properties of $La_{1-x}A'_xMnO_3$ (A' = Sr, Ce, Hf)

TAIHEI NITADORI,[1] SHIGEO KURIHARA,[2] AND MAKOTO MISONO[3]

Department of Synthetic Chemistry, Faculty of Engineering, The University of Tokyo, Bunkyo-ku, Tokyo 113, Japan

Received March 29, 1985; revised October 17, 1985

Catalytic activities of perovskite-type mixed oxides ($La_{1-x}A'_xMnO_3$, where A' = Sr, Ce, Hf and x = 0–1.0) for oxidation of propane have been measured and they were compared with several properties of oxygen of the catalysts. It was found that the catalytic activity of $La_{1-x}Sr_xMnO_3$ varied in parallel with the reducibility of catalyst surface, the amount of reversibly adsorbed oxygen (static measurement and low-temperature peak of temperature-programmed desorption (TPD)), and the rate of isotopic equilibration of oxygen. However, the high-temperature peak of TPD was not correlated with the catalytic activity. The reasons for the parallel variation of these properties have been discussed on the basis of the possible nonstoichiometry and the surface properties of catalysts. Similar effects of Ce and Hf substitution were assumed to be due to the formation of cation vacancy at A site.

INTRODUCTION

Perovskite-type mixed oxides (ABO_3) have a well-defined bulk structure and the composition of cations at both A and B sites can be variously changed (*1*). Therefore, these mixed oxides are suitable materials for the study of the structure–property relationship of catalysts. Furthermore, they are efficient catalysts in practical uses like catalytic combustion (*2–4*). Other catalytic reactions have also been reported (*5*).

We previously reported the effects of Sr^{2+} and Ce^{4+} substitution for La in $LaCoO_3$ and $LaFeO_3$ on the catalytic activity for oxidation and related properties (*6–8*). In the present work, we investigated the effects of Sr^{2+}, Ce^{4+}, and Hf^{4+} substitition in $LaMnO_3$, since $LaMnO_3$ shows a relatively high catalytic activity (*2–4*) and nonstoichiometry (excess oxygen) which is different from $LaCoO_3$ and $LaFeO_3$ (*9*). We attempted to elucidate the relationship between the catalytic properties and the composition of the catalyst, placing emphasis on the reactivities of oxygen both in the bulk and on the surface.

[1] Present address: Japan Tabacco Inc.

[2] Present address: Dentsu Inc.

[3] To whom correspondence should be addressed.

EXPERIMENTAL

Catalysts

$La_{1-x}Sr_xMnO_3$ and $La_{1-x}Ce_xMnO_3$ catalysts were prepared from mixtures of metal acetates in the same manner as described in the previous paper (*6, 8*). $La_{1-x}Hf_xMnO_3$ catalysts were prepared from mixtures of lanthanum nitrate, manganese nitrate, and hafnium oxide. CeO_2 (surface area, 3.7 m^2/g) and HfO_2 (8.4 m^2/g) were prepared by calcination at 850°C of acetate and oxide, respectively. Powder X-ray diffraction (XRD) patterns were recorded on an X-ray diffractometer (Rigaku Denki, Rotaflex, RU-200) using CuK radiation. Surface area was measured by BET method (N_2 adsorption). XPS was recorded on ESCA 750 (Shimadzu).

Apparatus

Conventional flow, pulse, and closed circulation systems as described before (*6–8*) were employed.

Procedure

(*1*) *Oxidation of propane.* The catalytic oxidation of propane (227°C) was carried out with the flow system. Prior to each reaction, the catalysts (300 mg) were treated

0021-9517/86 $3.00

in an O_2 stream for 1 h at 300°C. A gas mixture of propane (0.83%), O_2 (33.3%), and N_2 (balance) was fed in a flow reactor. The flow rate of the mixed gas was 60 cm^3 min^{-1}. Products were analyzed by a gas chromatograph (silica gel, 1 m, kept at 84°C).

(2) Reduction of catalysts by CO. The reduction of the catalysts by CO was conducted in the pulse reactor. Prior to the reaction, the catalysts (50 mg) were heated in an O_2 stream for 1 h at 300°C. The flow rate of carrier gas (He) was 30 cm^3 min^{-1} and the size of each pulse was usually 0.1 cm^3. Products were analyzed by a gas chromatograph (WG-100, Gasukuro Kogyo Inc., 60°C).

(3) Temperature-programmed desorption (TPD) of oxygen. TPD of oxygen was carried out with a flow system using helium as a carrier gas. Prior to each run, the samples (1 g) were treated in an O_2 stream for 1 h at 800°C. Oxygen impurity in He was removed by a molecular sieve 5A kept at the temperature of liquid nitrogen. After they were cooled to room temperature, a helium stream was substituted for an O_2 stream. Then the temperature of the sample was raised at a constant rate of 20 deg min^{-1} up to 800°C and oxygen desorbed was detected by use of a quadrupole mass spectrometer (NEVA, NAG-531). Only oxygen was detected in the desorbed gas. It was confirmed for $LaMnO_3$ and $La_{0.8}Sr_{0.2}MnO_3$ that TPD curves were reproduced in the repeated runs after the same treatment.

(4) Isotopic exchange and equilibration of oxygen. ^{18}O-Exchange between O_2 and perovskite, and ^{18}O-equilibration of O_2 in the gas phase were conducted in the closed-circulation system. The samples (300 mg) were pretreated with circulating pure O_2 (100 Torr) at 300°C (with a trap kept at liquid-nitrogen temperature) and subsequently evacuated for 1 h at 300°C. O_2 enriched in ^{18}O (70–75%) was prepared by mixing $^{18}O_2$ (99.5%), purchased from Japan Radioisotope Associations, and pure $^{16}O_2$. ^{18}O-Distribution in O_2 in the gas phase was analyzed by a mass spectrometer (Hitachi, RUM-S) after intermittent sampling.

(5) Adsorption of oxygen. First, the catalysts (1 g) were heated in O_2 (ca. 20 Torr) at 300°C for 1 h. After the system was evacuated at 300°C for 0.5 h, oxygen was introduced at 300°C. Then the temperature was lowered stepwise to 200, 100, and 25°C in the presence of O_2 (ca. 10 Torr). The amounts of oxygen uptake at each temperature were cumulatively measured. At each temperature, the amount of reversible oxygen uptake was also measured, by evacuating the sample for 0.5 h. The latter oxygen will be called reversibly adsorbed oxygen.

RESULTS

Structure and Surface Area of Catalysts

The surface area and crystal structure of the catalysts prepared are summarized in Table 1. The structure of the samples was examined with reference to ASTM cards. In the range of $0 \leq x \leq 0.4$, $La_{1-x}Sr_xMnO_3$ had the perovskite structure. The XRD patterns of $SrMnO_3$ ($x = 1.0$) was consistent with that of four-layer hexagonal $SrMnO_3$ which was reported by Negas and Roth *(10)*. In the range of $0.6 \leq x \leq 0.8$, $La_{1-x}Sr_xMnO_3$ consisted of the perovskite-

TABLE 1

Surface Area and Structure of Catalysts

Catalyst	Calcination		Surface area (m^2/g)	Structure
	Temp., °C	Time, h		
$LaMnO_3$	850	5	2.4	P[a]
$La_{0.8}Sr_{0.2}MnO_3$	850	5	4.2	P
$La_{0.6}Sr_{0.4}MnO_3$	850	5	4.7	P
$La_{0.4}Sr_{0.6}MnO_3$	850	5	5.7	P + H[b]
$La_{0.2}Sr_{0.8}MnO_3$	850	5	5.5	P + H
$SrMnO_3$	950	7	1.4	H
$La_{0.9}Ce_{0.1}MnO_3$	850	10	4.4	P + CeO_2
$La_{0.8}Ce_{0.2}MnO_3$	850	10	4.0	P + CeO_2
$La_{0.6}Ce_{0.4}MnO_3$	850	10	4.0	P + CeO_2
$La_{0.4}Ce_{0.6}MnO_3$	850	10	8.2	P + CeO_2
$La_{0.9}Hf_{0.1}MnO_3$	850	10	4.6	P + HfO_2
$La_{0.8}Hf_{0.2}MnO_3$	850	10	10.2	P + HfO_2
$La_{0.6}Hf_{0.4}MnO_3$	850	10	5.2	P + HfO_2

[a] Perovskite structure.
[b] Hexagonal $SrMnO_3$(ABAC-type) structure.

type structure and a small portion of hexagonal $SrMnO_3$; the latter increased with x. Here, unless stated explicitly, the perovskite catalysts are denoted by the nominal compositions, neglecting the mixed phases and nonstoichiometry.

In the case of $La_{1-x}A'_xMnO_3$ (A' = Ce or Hf), CeO_2 or HfO_2 phase appeared, besides the perovskite phase. XRD peaks of CeO_2 or HfO_2 phase increased with increase in x. But XRD lines due to La_2O_3 and Mn_2O_3 were not detected. By comparison with the XRD intensities of pure CeO_2 and Mn_2O_3, it was indicated that about a half of Ce was present as CeO_2 and the amount of Mn_2O_3 was less than one-tenth of CeO_2 in the case of $La_{0.9}Ce_{0.1}MnO_3$. The amount of CeO_2 changed little when $La_{0.9}Ce_{0.1}MnO_3$ was calcined at 1000°C for 10 h.

Oxidation of Propane

The catalytic activities of $La_{1-x}Sr_xMnO_3$ ($0 \leq x \leq 1.0$) for propane oxidation at 227°C are shown in Fig. 1, in which the rates are normalized to unit surface area which are given in Table 1. The oxidation activity increased gradually with the Sr^{2+} substitution at first, but decreased at higher extents of the substitution, showing a maximum at x = 0.6. This trend is different from that observed for Fe or Co systems, in which the activity increased remarkably by the substitution of only a small amount of Sr (*6–8*).

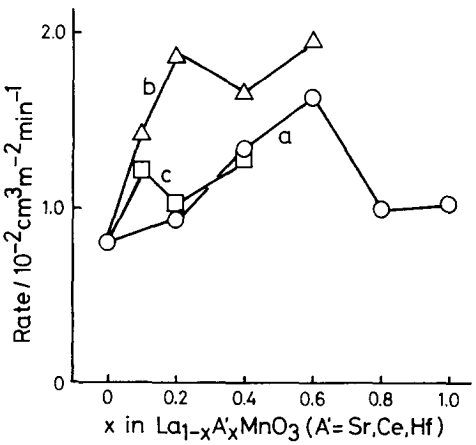

FIG. 1. Effects of Sr^{2+}-, Ce^{4+}-, and Hf^{4+}-substitution on the catalytic activity of $LaMnO_3$ for oxidation of propane at 227°C. (a) Sr^{2+}, (b) Ce^{4+}, (c) Hf^{4+}.

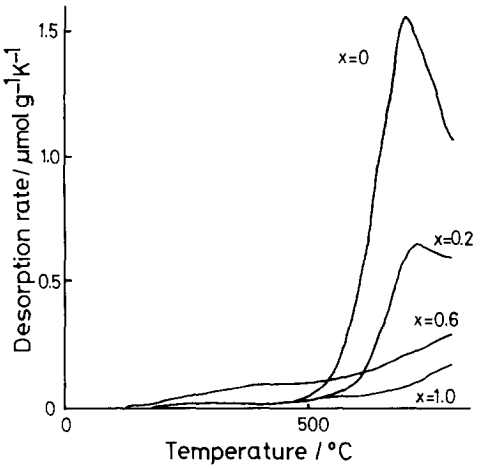

FIG. 2. TPD profiles of oxygen from $La_{1-x}Sr_xMnO_3$ (x = 0–1.0).

The activities of $La_{1-x}A'_xMnO_3$ (A' = Ce or Hf) for propane oxidation are also shown in Fig. 1. The effect of Ce^{4+} or Hf^{4+} substitution on propane oxidation was a little greater than the Sr^{2+} substitution. Catalytic activities of CeO_2 and HfO_2 were very low (lower by a factor of 10^2 than $La_{0.9}Ce_{0.1}MnO_3$) and therefore a mixture of $La_{0.9}Ce_{0.1}MnO_3$ + CeO_2 (9 : 1) showed the same activity as the former alone within experimental error.

TPD of Oxygen

Figure 2 shows TPD of oxygen from $La_{1-x}Sr_xMnO_3$ (x = 0, 0.2, 0.6, and 1.0), where the rates of desorption calculated from the oxygen concentration in the eluant gas are plotted against the catalyst temperature. A broad and small peak appeared at the relatively low temperature range (300–500°C) for all of four samples. The amounts of oxygen desorbed below 500°C (low temperature peak) were 0.12 ml(NTP) g^{-1} (x = 0), 0.16(0.2), 0.48(0.6), and 0.12(1.0), respectively. A maximum value was obtained for x = 0.6. Even for x = 0.6, the amount was only about half of the surface monolayer of oxygen. This is in marked contrast to the Co and Fe systems (*6, 8*). At the

higher temperature range, in the cases of $LaMnO_3$ and $La_{0.8}Sr_{0.2}MnO_3$, large peaks appeared at 700 and 730°C, respectively. $La_{0.4}Sr_{0.6}MnO_3$ showed a high-temperature peak at 830°C, whose peak height was fairly smaller than that of $La_{0.8}Sr_{0.2}MnO_3$. In the case of $SrMnO_3$, the high-temperature peak probably existed above 850°C, because the TPD curve gradually increased up to 850°C. Therefore, the high-temperature peak shifted to a higher temperature and the peak height became lower with increase of x. This trend is also in contrast to that of the Co and Fe systems. In the latter systems, the desorption of O_2 increased monotonously with x, and TPD curves were more or less similar with one another (*6*, *8*).

TPD profiles for $La_{1-x}A'_xMnO_3$ (A' = Ce, Hf; x = 0.1, 0.4) are shown in Fig. 3. TPD profiles from the four samples were similar to $La_{0.8}Sr_{0.2}MnO_3$, having small peaks at lower temperatures and large peaks at higher temperatures. The amount of desorbed oxygen of low-temperature peak was greater for x = 0.4 than for x = 0 and 0.1 for both the Ce and Hf substitution.

Isotopic Exchange of Oxygen

Figure 4 shows the results of isotopic equilibration in the gas phase and exchange

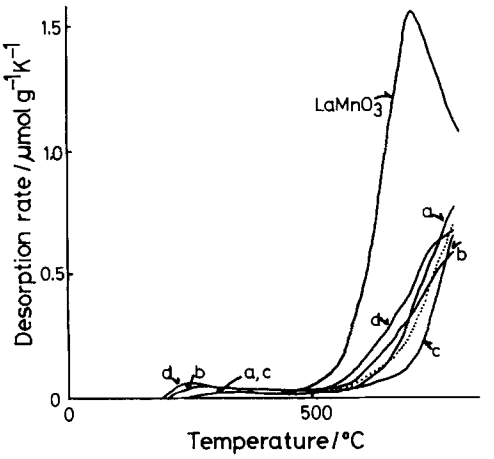

FIG. 3. TPD profiles of oxygen from $La_{1-x}A'_xMnO_3$ (A' = Ce, Hf) and $La_{0.9}MnO_3$. (a) $La_{0.9}Ce_{0.1}MnO_3$, (b) $La_{0.6}Ce_{0.4}MnO_3$, (c) $La_{0.9}Hf_{0.1}MnO_3$, (d) $La_{0.6}Hf_{0.4}MnO_3$. Dotted line: $La_{0.9}MnO_3$.

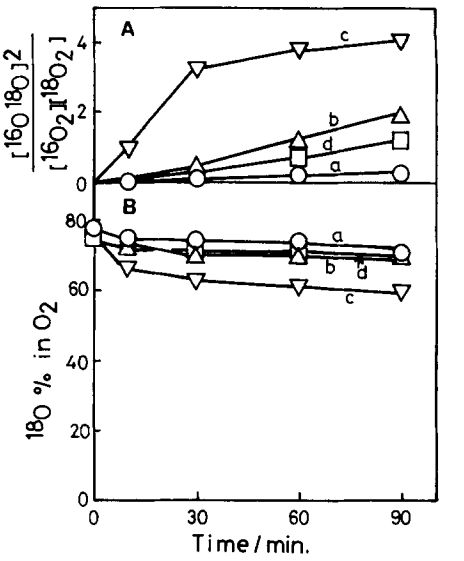

FIG. 4. Isotopic exchange of oxygen from $La_{1-x}Sr_xMnO_3$ at 300°C. (A) Equilibration in the gas phase. (B) Exchange between gaseous and lattice oxygen. (a) x = 0, (b) 0.2, (c) 0.6, (d) 1.0.

between gaseous and catalyst oxygen for $La_{1-x}Sr_xMnO_3$ ($0 \leq x \leq 1.0$). The rate of isotopic equilibration was $x = 0.6 > 0.2 \sim 1.0 > 0$ (Fig. 4A). On the other hand, as Fig. 4B shows, the isotopic exchange proceeded very slowly over all samples. When the exchange rates are expressed, as in the previous paper (*8*), by the amount of lattice oxygen which would have had the same isotopic composition as in the gas phase, the rates of exchange were only about 0.7–0.9 layers after 90 min. These were much smaller than those for the previous systems (*6*, *8*). The exchange seems to be limited only to the oxygen on the surface or very near the surface in the case of the Mn system.

Results of isotope experiments over $La_{1-x}A'_xMnO_3$ (A' = Ce, Hf; x = 0.1, 0.4) are shown in Fig. 5. Equilibration rate increased by both Ce and Hf substitution. It is noticed in the case of the Ce system that the exchange rates remarkably increased with increasing x. The rates were about 3 and 16 layers after 90 min for x = 0.1 and 0.4, respectively. This is comparable with

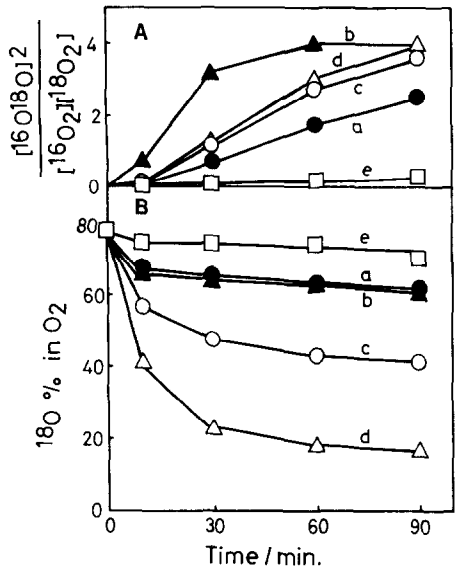

FIG. 5. Isotopic exchange of oxygen over $La_{1-x}A'_xMnO_3$ (A' = Ce, Hf; x = 0.1, 0.4). (A) Equilibration in the gas phase. (B) Exchange between gaseous and lattice oxygen. (a) $La_{0.9}Hf_{0.1}MnO_3$, (b) $La_{0.6}Hf_{0.4}MnO_3$, (c) $La_{0.9}Ce_{0.1}MnO_3$, (d) $La_{0.6}Ce_{0.4}MnO_3$, (e) $LaMnO_3$.

$La_{1-x}Ce_xCoO_3$ (*8*). Due to the rapid isotopic exchange the isotopic equilibration for $La_{0.6}Ce_{0.4}MnO_3$ apparently became lower as in the Fe system (*8*). Isotopic equilibration over CeO_2 and HfO_2 was much slower than $LaMnO_3$.

Reducibility of Catalyst by CO

Figure 6 shows the results of reduction of $La_{1-x}Sr_xMnO_3$ by CO pulses at 300°C. The ordinate indicates the percentage conversion of CO to CO_2 for repeated pulses, and the abscissa is the sum of CO_2 formed from that pulse and the precedings. The sum of CO_2 formed (abscissa) corresponds to the extent of the reduction of the catalysts at each pulse. It is noted that $La_{1-x}Sr_xMnO_3$ was reduced more easily when x increased initially, but the reducibility showed a maximum for $La_{0.4}Sr_{0.6}MnO_3$ and then declined. The amount of CO_2 formed for the first three pulses was comparable with the number of oxygen atoms on the surface monolayer for x = 0.6, and was much less for the others. When Ce^{4+} or Hf^{4+} was partially

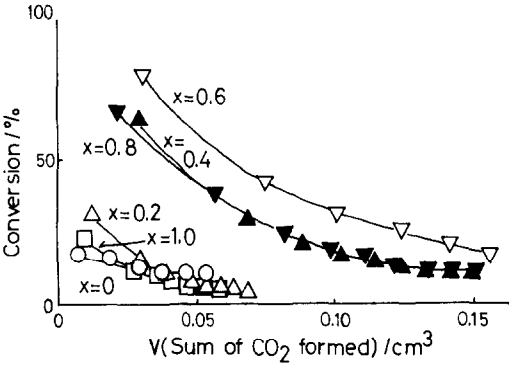

FIG. 6. Reduction of $La_{1-x}Sr_xMnO_3$ by CO pulses at 300°C. Catalyst weight, 50 mg; CO pulse size, 0.1 cm^3.

substituted for La, the catalyst also became easier to be reduced (Fig. 7).

Reversible Adsorption of Oxygen

Table 2 summarizes the amounts of adsorbed oxygen for x = 0 and 0.6, where each catalyst was preevacuated at 300°C. The difference between the values *in vacuo* and in O_2 correspond to the reversible adsorption at each temperature. The reversible adsorption increased with the increase of temperature and was greater for x = 0.6 than for x = 0 at 300°C. This result was in agreement with TPD results (see the amount of desorbed oxygen in the range of 200–500°C), although the results in Table 2 are of equilibrium property and the TPD results are of kinetic one.

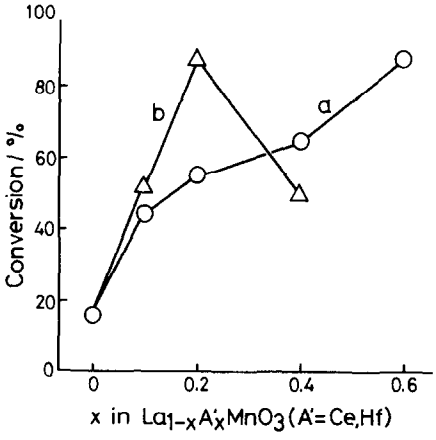

FIG. 7. Reduction of $La_{1-x}A'_xMnO_3$ (A' = Ce, Hf) by the first CO pulse at 300°C. (a) Ce^{4+}, (b) Hf^{4+}.

TABLE 2

Adsorption of Oxygen by $La_{1-x}Sr_xMnO_3$ (x = 0, 0.6)

x		Temperature, °C			
		25	100	200	300
0	*In vacuo*[a]	18.1	14.5	8.7	0
	In oxygen[b]	18.1	14.5	13.7	9.7
0.6	*In vacuo*	72.1	72.1	57.2	0
	In oxygen	72.1	72.1	62.0	48.9

Note. These values are the amounts of oxygen with reference to that *in vacuo* at 300°C (10^{-3} ml g^{-1}).

[a] ca. 10^{-4} Torr.

[b] ca. 10 Torr.

DISCUSSION

Structure and Stoichiometry

It was reported that by the calcination in air at 1350°C (*11*) $La_{1-x}Sr_xMnO_3$ with perovskite structure was formed in the range of $0 \leq x \leq 0.7$, the structure becoming anion-deficient ($La_{1-x}Sr_xMnO_{3-\delta}$) for $0.4 \leq x \leq 0.7$. It was also reported that perovskite structure was formed for $0 \leq x \leq 0.8$ (anion-deficient structure for $0.7 \leq x \leq 0.8$) when calcined at 1100°C in air (*12*). The samples used in the present investigation had a single perovskite structure in the range of $0 \leq x \leq 0.4$, four-layer hexagonal structure for $x = 1.0$, and mixtures of a large portion of perovskite and a small portion of hexagonal phase for $0.6 \leq x \leq 0.8$. The range of a single perovskite phase was narrower in the present work probably due to the relatively low calcination temperature (850°C).

As for the nonstoichiometry, excess oxygen (probably cation vacancy instead of interstitial oxygen) was reported for $x = 0$ (*9*, *13*), besides the above-mentioned oxygen vacancy for high x values. The presence of excess oxygen is understandable by the tendency of Mn to achieve the +4 state. Tofield and Scott (*9*) reported that $LaMnO_{3.12}$ was formed after calcination in air at 1100–1200°C. This oxidative nonstoichiometry is in agreement with the present data of TPD. The amount of oxygen desorbed from $LaMnO_3$ up to 800°C was 6.0 ml g^{-1} (5.9 ml g^{-1} at 500–800°C) (Fig. 2), which is close to the value expected for the reduction of $Mn^{4+} \rightarrow Mn^{3+}$ of $LaMnO_{3.12}$ (*9*) (5.4 ml g^{-1}; $LaMnO_{3.12} \rightarrow LaMnO_3 + 0.06\ O_2$). Therefore, the high-temperature peak (700°C) in TPD profile for $LaMnO_3$ is assignable to desorption of excess oxygen accompanied by the reduction of Mn^{4+} to Mn^{3+}. In other words, $LaMnO_3$ used in the present study had a comparable amount of excess oxygen (or Mn^{4+}) with that reported (*9*).

The composition for $x = 0$ was suggested to be $La_{0.94}Mn_{0.98}O_3$ by Tofield and Scott (*9*), but no reliable data for the structure of Sr-substituted lanthanum manganite has been reported. However, if one considers that the amount of Mn^{4+} was reported to increase with x (*11*, *12*) and that oxygen vacancy was formed for high x values as described above, it appears probable that the cation vacancies which were present for $x = 0$ gradually decreased by the Sr substitution and at a certain x value the structure became oxygen-deficient. This explains qualitatively the trend observed for low-temperature TPD peak shown in Fig. 2, as well as the trend of the catalytic activity (see below). The amount of oxygen desorbed up to about 800°C decreased and the high-temperature peak shifted to higher temperatures with increase in x, indicating that the reduction of Mn^{4+} to Mn^{3+} was suppressed by doped Sr^{2+}. This is consistent with the fact that $SrMnO_3$ was thermally very stable and showed smallest amount of O_2 desorption.

All of the Ce^{4+}- and Hf^{4+}-substituted samples prepared in the present work contained both perovskite and CeO_2 or HfO_2 phase, and therefore the substitution ratio of Ce^{4+} or Hf^{4+} in the perovskite phase was not quantitatively known. However, since the amounts of La_2O_3 or Mn_2O_3 phases were much less than CeO_2, the major components of these samples are likely close to $La_{1-x}A'_{x-y}\phi_yMnO_3$ (A' = Ce, Hf; $1 > x > y > 0$; ϕ = A-site cation vacancy).

Comparison of Reactivity of Oxygen and Catalytic Activity

Effects of Sr substitution. The changes of the catalytic activity for oxidation and related properties which were brought about by the Sr substitution of $LaMnO_3$ are compared in Fig. 8. Parallel variation of these properties may be obvious in this figure, all the values being maximal at $x = 0.6$. That is to say, a factor common in (i) the oxidation power of catalyst (expressed by percentage conversion of CO), (ii) the amount of oxygen which is easily adsorbed or desorbed at about 300°C (the amount of reversibly adsorbed oxygen at 300°C, or oxygen desorbed in TPD at low temperatures), and (iii) the capability of the surface for dissociation of O_2 (rate of isotopic equilibration of O_2) is the controlling factor of the catalytic activity for oxidation.

Among these three properties, as described in the Results section, the amounts of oxygen utilized for oxidation of CO, (i), and for reversible adsorption, (ii), were comparable or less than surface monolayer, in contrast to the Co and Fe systems. The isotopic equilibration, (iii), is the process which takes place on the surface. Therefore, all three properties concerning oxygen are surface properties. The rate of isotopic exchange seems to vary in a similar way (Fig. 4), but the trend was not obvious since the exchange was very slow. This exchange is also limited only to the surface.

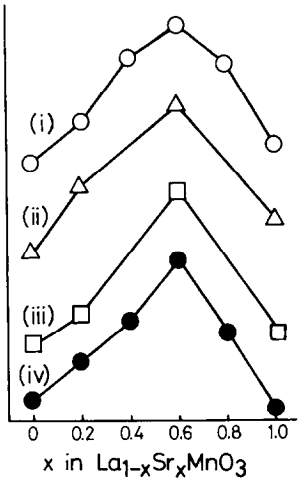

FIG. 8. Changes of the catalytic activity for oxidation and related properties which were brought by the Sr substitution of $LaMnO_3$. (i) Percentage conversion of CO (Fig. 6). (ii) The amount of reversibly adsorbed oxygen at 300°C (Table 2 and Fig. 2). (iii) Rate of isotopic equilibration of O_2 (Fig. 4A). (iv) Rate of propane oxidation at 227°C. (These values are all normalized to catalyst weight.)

The high-temperature peak may be considered to reflect the bulk properties as discussed in the previous section, but it is not correlated with the properties (i) (iii) given in Fig. 8. For example, the high-temperature peak of TPD from the sample with $x = 0.2$ was less than half of the amount from the sample with $x = 0$ (Fig. 2), while equilibration rate was higher for $x = 0.2$ than for $x = 0$ (Fig. 4). Thus, it may be concluded that the catalytic activity of $La_{1-x}Sr_xMnO_3$ is primarily correlated not with the bulk properties but with the surface properties.

The reason why those properties in Fig. 8 change in parallel showing maxima at $x = 0.6$ are discussed in the following. Although further investigation is necessary to elucidate the reason satisfactorily, the following may be pointed out. As discussed in the previous section, the excess oxygen which is present for $x = 0$ decreases with increasing x and finally the structure becomes oxygen-deficient for high values of x. This indicates that, as the x value increases, surface oxide ion tends to desorb, forming coordinatively unsaturated *B*-site ion on the surface. The easier desorption of oxygen may reflect in the increase of the low-temperature peak, the reversibly adsorbed oxygen and the oxidation power of catalyst. The increase of the coordinatively unsaturated Mn ions may explain the increases of the equilibration rate, and the catalytic avtivity. The change of those properties and catalytic activity above $x = 0.6$ is probably caused by the presence of $SrMnO_3$ phase. It is also probable that part of the surface for $x \geq 0.6$ was covered by a less active Sr-rich phase, although preliminary XPS measurements showed only monotonous increase of Sr content of the surface with x.

Effects of Ce or Hf substitution. As discussed above, the compositions of the catalysts containing Ce^{4+} or Hf^{4+} are probably the mixture of $La_{1-x}A'_y\phi_{x-y}MnO_3$ (A' = Ce, Hf) having A-site cation vacancies, and CeO_2 or HfO_2. The properties measured in this study are due to the mixed oxides, since CeO_2 and HfO_2 themselves were much less active for catalytic oxidation and isotopic equilibration of oxygen. If A-site vacancies are formed, a part of trivalent Mn ion in perovskite structure changes to tetravalent to compensate the A-site vacancy, so that the anion vacancy is possibly formed for larger x values. This is essentially the same effects as Sr substitution. Therefore, the effect of the Ce^{4+} or Hf^{4+} substitution is expected to be similar to that of Sr^{2+} substitution. This is supported by the similarity of the TPD profiles (compare Figs. 2 and 3), as well as by the increased reducibilities (Fig. 7) and catalytic activities (Fig. 1). To examine the effect of A-site vacancy, a sample was prepared from a nonstoichiometic mixture of La and Mn salts (La/Mn = 0.9 in atomic ratio). Since it showed XRD peaks only from perovskite-type structure, the structure was supposed to be $La_{0.9}\phi_{0.1}MnO_3$. As expected, TPD of oxygen (dotted line in Fig. 3) of this sample was similar to those of $La_{0.9}Hf_{0.1}MnO_3$ and $La_{0.9}Ce_{0.1}MnO_3$.

The accelerated isotopic equilibration for Ce- and Hf-substituted $LaMnO_3$ (Fig. 5A) and $La_{0.9}MnO_3$ may be understood in a similar way. However, the reason why remarkable acceleration of isotopic exchange was observed only for Ce substitution (Fig. 5B) is not known at present. One possibility is that more anion vacancies are formed without formation of inert phase on the surface.

ACKNOWLEDGMENTS

This work was supported in part by the Grant-in-Aid from the Ministry of Education, Science and Culture. Helpful discussion with Dr. J. Mizusaki, concerning the structure, is gratefully acknowledged.

REFERENCES

1. Voorhoeve, R. J. H., "Advanced Materials in Catalysis," p. 129. Academic Press, New York, 1977.
2. Libby, W. F., *Science (Washington, D.C.)* **171,** 499 (1971).
3. Voorhoeve, R. J. H., Remeika, J. P., Freeland, P. E., and Mattias, B. T., *Science (Washington, D.C.)* **177,** 353 (1972).
4. Nakamura, T., Misono, M., Uchijima, T., and Yoneda, Y., *Nippon Kagaku Kaishi 1980,* 1679.
5. Ichimura, K., Inoue, Y., and Yasumori, I., *Bull. Chem. Soc. Japan* **54,** 1787 (1981); Damme, H. V., and Hall, W. K., *J. Catal.* **69,** 371 (1981); Lombardo, E. A., Tanaka, K., and Toyoshima, I., *J. Catal.* **80,** 340 (1983); Tascón, J. M. D., Mendioroz, S., and Tejuca, L. G., *Z. Phys. Chem. NF.* **124,** 109 (1981); Arakawa, T., Tsuchiya, S., Shiokawa, J., *J. Catal.* **74,** 317 (1982).
6. Nakamura, T., Misono, M., and Yoneda, Y., *Bull. Chem. Soc. Japan* **55,** 394 (1982).
7. Nakamura, T., Misono, M., and Yoneda, Y., *J. Catal.* **83,** 151 (1983); *Chem. Lett., 1981,* 1589.
8. Nitadori, T., and Misono, M., *J. Catal.* **93,** 459 (1985).
9. Tofield, B. C., and Scott, W. R., *J. Solid State Chem.* **10,** 183 (1974).
10. Negas, T., and Roth, R. S., *J. Solid State Chem.* **1,** 409 (1970).
11. Jonker, G. H., and Van Santen, J. H., *Physica* **16,** 337 (1950).
12. Shimizu, T., and Moriwaka, Y., *Nippon Kagaku Kaishi 1978,* 1462.
13. Kamegashira, N., Miyazaki, Y., and Yamamoto, H., Materials Chemistry and Physics, **11,** 187 (1984).